J Paleolimnol (2009) 42:401–412
DOI 10.1007/s10933-008-9284-5

ORIGINAL PAPER

Age modeling of young non-varved lake sediments: methods and limits. Examples from two lakes in Central Chile

Lucien von Gunten · Martin Grosjean · Jürg Beer · Philipp Grob · Arturo Morales · Roberto Urrutia

Received: 15 July 2008 / Accepted: 20 November 2008 / Published online: 9 December 2008

Abstract High-resolution and highly precise age models for recent lake sediments (last 100–150 years) are essential for quantitative paleoclimate research. These are particularly important for sedimentological and geochemical proxies, where transfer functions cannot be established and calibration must be based upon the relation of sedimentary records to instrumental data. High-precision dating for the calibration period is most critical as it determines directly the quality of the calibration statistics. Here, as an example, we compare radionuclide age models obtained on two high-elevation glacial lakes in the Central Chilean Andes (Laguna Negra: 33°38′S/70°08′W, 2,680 m a.s.l. and Laguna El Ocho: 34°02′S/70°19′W, 3,250 m a.s.l.). We show the different numerical models that produce accurate age-depth chronologies based on ^{210}Pb profiles, and we explain how to obtain reduced age-error bars at the bottom part of the profiles, i.e., typically around the end of the 19th century. In order to constrain the age models, we propose a method with five steps: (i) sampling at irregularly-spaced intervals for ^{226}Ra, ^{210}Pb and ^{137}Cs depending on the stratigraphy and microfacies, (ii) a systematic comparison of numerical models for the calculation of ^{210}Pb-based age models: constant flux constant sedimentation (CFCS), constant initial concentration (CIC), constant rate of supply (CRS) and sediment isotope tomography (SIT), (iii) numerical constraining of the CRS and SIT models with the ^{137}Cs chronomarker of AD 1964 and, (iv) step-wise cross-validation with independent diagnostic environmental stratigraphic markers of known age (e.g., volcanic ash layer, historical flood and earthquakes). In both examples, we also use airborne pollutants such as spheroidal carbonaceous particles (reflecting the history of fossil fuel emissions), excess atmospheric Cu deposition (reflecting the production history of a large local Cu mine), and turbidites related to historical earthquakes. Our results show that the SIT model constrained with the ^{137}Cs AD 1964 peak performs best over the entire chronological profile

L. von Gunten (✉) · M. Grosjean · P. Grob
Oeschger Centre for Climate Change Research and Institute of Geography, University of Bern, Erlachstrasse 9a, Bern CH-3012, Switzerland
e-mail: lucien.vongunten@giub.unibe.ch

M. Grosjean
NCCR Climate, University of Bern, Bern CH-3012, Switzerland

J. Beer
Department of Surface Waters (SURF), Swiss Federal Institute of Aquatic Science and Technology (EAWAG), Dübendorf CH-8600, Switzerland

A. Morales
Superintendencia Geología-División El Teniente, CODELCO, Casilla, Santiago, Chile

R. Urrutia
Centro EULA-Chile, Universidad de Concepción, Casilla, Concepción, Chile

(last 100–150 years) and yields the smallest standard deviations for the sediment ages. Such precision is critical for the calibration statistics, and ultimately, for the quality of the quantitative paleoclimate reconstruction. The systematic comparison of CRS and SIT models also helps to validate the robustness of the chronologies in different sections of the profile. Although surprisingly poorly known and under-explored in paleolimnological research, the SIT model has a great potential in paleoclimatological reconstructions based on lake sediments.

Keywords Sedimentology · Paleolimnology · Radionuclides · Sediment isotope tomography · Calibration · South America

Introduction

High-resolution (annual to sub-decadal), well-calibrated, climate-state variables from natural paleoclimatic archives are pre-requisites to establish robust climate reconstructions at regional to global scales (Jones and Mann 2004; Luterbacher et al. 2004; Moberg et al. 2005). Such variables are, ultimately, the scientific basis to quantitatively assess natural forced and unforced climate variability of the past, detect recent anthropogenic climate change, and evaluate statistics of extreme events. High-resolution paleoclimatic data with known and, ideally, small uncertainties help significantly to reduce uncertainties of future climate change (Hegerl et al. 2006).

Lake sediments are valuable paleoclimate archives, especially because of their potential to preserve both the high and the low frequency components of climate variability, and to provide very long records (Moberg et al. 2005). However, lake sediment records are rarely used for quantitative regional, global, or inter-hemispherical comparisons (Jones and Mann 2004; Luterbacher et al. 2004; Moberg et al. 2005). Whereas tree-rings, documentary data (e.g., historical chronicles), ice core and coral data sets are widely used in such reconstructions, only very few lake-sediment data sets meet the quality requirements for such purposes. Lake sediments do not systematically provide: (i) seasonal to annual temporal resolution, (ii) significant correlation with instrumental data (precipitation, temperature …), (iii) known statistical uncertainties and reduced errors of the reconstructed variable, and (iv) well-dated, long records.

Typically, geochemical or taxonomic analysis of sedimentary constituents is very time-consuming. Millennial-long annually resolved time series could not be produced. However, new rapid non-destructive scanning techniques (Zolitschka et al. 2001) have the potential to generate large proxy data sets from lake sediments. However, it is often difficult to develop paleoclimate records from such proxies. For example, Transfer Functions ("calibration space for time", Birks 1998) cannot be applied to geochemical proxies because a modern training set cannot be established due to the heterogeneity of settings in different catchments. Therefore, "calibration in time", that is correlation with instrumental records, needs to be applied for geochemical sediment proxies if they are used for quantitative paleoclimate reconstructions. Obviously, high-precision dating of lake sediments during the time with instrumental meteorological data series (typically the last 100–150 years) is fundamental for such purposes. Often, the calibration period is limited by relatively short instrumental records, which is most critical if it needs to be split into two parts (calibration and cross-validation of the calibration) to estimate the error of the calibration statistics (Cook et al. 1994). That is the reason why the full range of the calibration period must be used. In consequence, high-precision dating is essential for the entire temporal range of the calibration, in particular for the beginning of the instrumental period (typically the end of the 19th century). Unfortunately, that is exactly the time when ^{210}Pb-based chronologies show the largest uncertainties.

In non-varved lake sediments younger than ca. 150 years, ^{210}Pb radiochronology (Krishnaswamy et al. 1971; Robbins 1978; Appleby 2000, 2001, 2008) is the common "dating" technique, often combined with discrete stratigraphic chronomarkers such as (i) ^{137}Cs peaks (AD 1963–1964), and the Chernobyl AD 1986 peak (Pennington et al. 1973; Ritchie et al. 1973; Albrecht et al. 1998; Abril 2004), (ii) peaks of spheroidal carbonaceous particle (SCP) profiles (Renberg and Wik 1984, 1985; Rose et al. 1999), and (iii) historical flood, earthquake or volcanic ash layers (e.g., Arnaud et al. 2002; Blass et al. 2007; Chapron et al. 2007; Boës and Fagel 2008). These events are discrete chronostratigraphic markers and do not provide continuous chronologies, which is

required for calibrations with instrumental records. Interpolation may not be appropriate for high-precision chronologies if sedimentation rates change in time.

In theory, radiometric ^{210}Pb activity profiles may provide continuous chronologies. Here the difficulty is that the ^{210}Pb activities have to be converted into numerical ages to obtain an age-depth model. Typically, one of the conceptual CFCS (constant flux constant sedimentation), CIC (constant initial concentration) or CRS (constant rate of supply) models (Appleby and Oldfield 1978; Robbins 1978; Appleby 2001, 2008) is used for this purpose. However, it is not *a-priori* known which of the models gives the best results. In most cases, variants of the CRS model are used. Usually, this model yields more realistic results than the CIC model (Oldfield et al. 1978; Appleby et al. 1979; Appleby 2008), although in some lakes the CIC model provides better results (e.g., Turner and Delorme 1996; Appleby 2001; Sonke et al. 2003). The model choice is often subjective and accepted if the result is consistent with the ^{137}Cs stratigraphic markers. Other than the CFCS and the CIC model, the CRS model can actually be constrained and forced through the AD 1964 peak (composite CRS model). Surprisingly, the pre-AD 1964 sediment ages are only very rarely validated, which is arguably not essential for many paleolimnological studies. But this is rather unfortunate as the lower part of the ^{210}Pb chronologies is often used to extrapolate sedimentation rates back to the beginning of the last millennium. This is the time when ^{14}C dating yields acceptable probability density functions for sediment ages (e.g., McCormac et al. 2004). Unfortunately, the time before the ^{210}Pb-dating range starts is precisely the period (Little Ice Age chronozone) with potentially the best chance to quantitatively assess natural climate variability (Bradley et al. 2003).

More recently, the inductive sediment isotope tomography model (SIT) has been introduced by Liu et al. (1991) to evaluate ^{210}Pb profiles in marine sediments. The SIT model has the advantage that it calculates sediment ages without *a-priori* assumption (such as CRS or CIC) and it can be applied when the sedimentation rate as well as the flux and the initial concentration of unsupported ^{210}Pb vary with time (Carroll et al. 1995; Carroll and Lerche 2003). Although tests with synthetic data have shown that the SIT model is a reliable alternative to the CRS and CIC models, it is surprisingly poorly recognized in the paleolimnological community and has, to our knowledge, only been used in a few limnological studies (Waugh et al. 1998; Carroll et al. 1999a, b).

In this paper we investigate two high-elevation proglacial lakes in the Central Chilean Andes and show how ^{210}Pb-based chronologies and their precision can be assessed and improved by a systematic ^{210}Pb model comparison. First we tested the unconstrained models (without stratigraphic markers). Subsequently we constrained the CRS and SIT models with the ^{137}Cs peak of AD 1964 and verified the continuous ^{210}Pb-chronologies with further site-specific independent discrete stratigraphic markers of known age. Ideally, these chronomarkers are well distributed across the time range of interest (last 150 years).

Study area, lake sediments and stratigraphic markers

Laguna Negra and Laguna El Ocho are high-elevation lakes in the western (windward) Central Chilean Andes. The studied area is located in the transition zone between the temperate, semi-arid, summer-warm (Csb) and the dry-cool high-mountain (E) climate (classification Köppen-Geiger), which is seasonally under subtropical (austral summer) or westerly (austral winter) influence. South-westerly winds predominate throughout the year (Miller 1976). The boundary-layer winds in the Andes, however, are confined through the W–E orientation of the valleys. This observation is important with regard to the transport and dispersal of pollutants, including SCPs and excess atmospheric Cu fallout. Laguna Negra is directly influenced by the urban and industrial history of Santiago, while Laguna El Ocho carries the fingerprint of the nearby Cu mine El Teniente.

Seismically, many large (>Mw 7) historical earthquakes have been observed during the past 150 years in the region (Barrientos 2007; Servicio sismologico de Chile 2008). Three of them were exceptionally strong, including the Great Chilean earthquake of AD 1960 (Mw 9.5) with the epicentre to the south of the study area (39°5′S), the earthquake AD 1906 (Mw 8.2) to the north of the study area

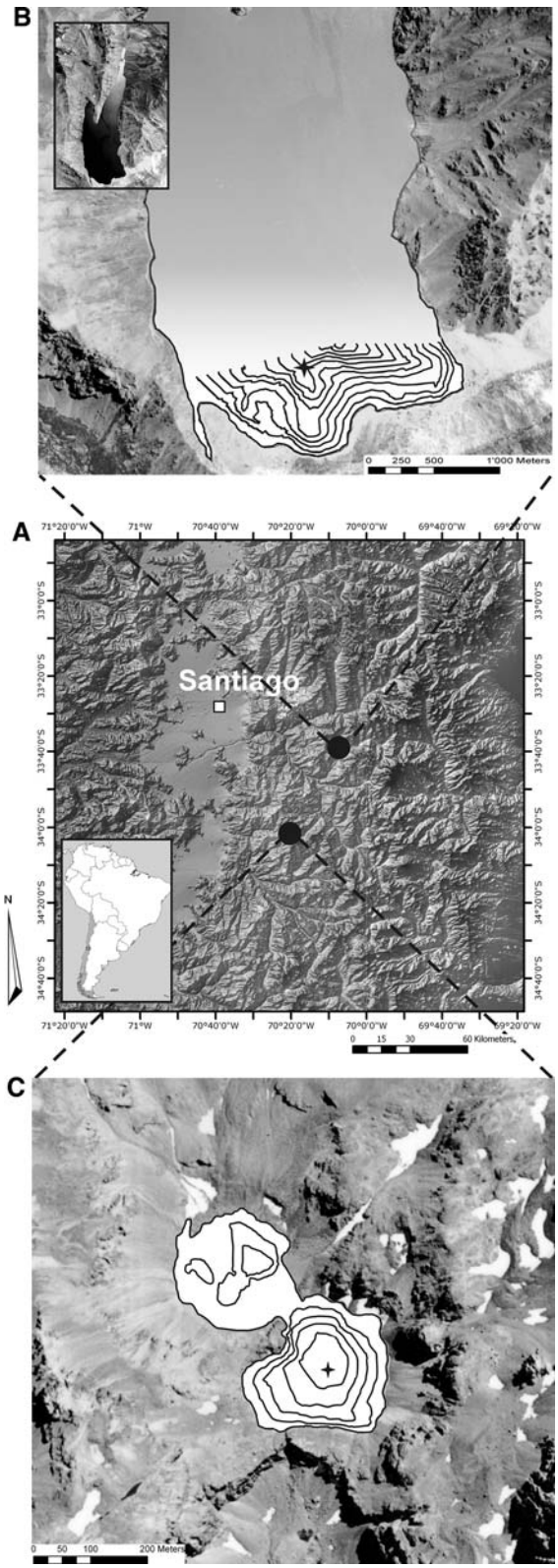

Fig. 1 **a** The study area with the location of both lakes and of ▶ the city Santiago de Chile. **b** Geographical setting, bathymetric map of Laguna Negra with the coring site; the bathymetric contour interval is 10 m. **c** Geographical setting, coring site and bathymetric map (isolines of 10 m) of Laguna El Ocho

(33°0′S), and the earthquake AD 1985 (Mw 8.0). The earthquake AD 1850 was not particularly strong (Mw 7.3) but had its epicentre directly in the area of the lakes (33.8°S/70.2°W). These earthquakes produced diagnostic marker layers in lake sediments from Central Chile (Chapron et al. 2007; Moernaut et al. 2007).

Laguna Negra

Laguna Negra (33°38′S/70°08′W, 2,680 m a.s.l., Fig. 1), located east of the city of Santiago de Chile (6.3 million people in 2006), is a large (5.73 km^2) and deep (>120 m) monomictic lake of combined glacial/landslide-dammed origin. It is oligotrophic, neutral (mean pH = 7.0), has a mean specific conductance of 131 µS cm^{-1} and is well oxygenated throughout the water column. Mean dissolved oxygen content was 8.2 mg l^{-1}, as measured along a 45 m profile on March 4, 2006. The catchment ranges up to 4,600 m a.s.l. and consists mainly of Oligocene to Miocene volcanites (andesites to basalt, dacite). Vegetation cover is very scarce (<10%, grasses and small shrubs).

The sediment core of Laguna Negra consists of four sedimentary facies (Fig. 2). Facies A1 is composed of dark greyish brown (4/2 2.5Y), massive fine to coarse silt (terminology after Munsell Color 1994). Facies A2 is a dark greyish brown (4/2 10YR) massive fine to coarse silt. Facies B is a massive silty interlayer with high organic content (C_{org} 3–4%) and macrofossil remains, mainly *Fissidens* water mosses. Facies C is a dark yellowish brown (4/6 10YR), massive, fine to coarse silt. Facies D is a gray (5/1 10YR), massive, fine to medium silt layer with fine to coarse stones.

The atmospheric pollution history of Laguna Negra, as indicated by the SCP profile, is dominated by the urban and industrial history of windward Santiago. Because of modern industrialisation and urban growth of Santiago in the 1850s–1860s (Rippy and Pfeiffer 1948; Mamalakis 1976; Ortega 1981), the occurrence of the first SCPs in the sediment

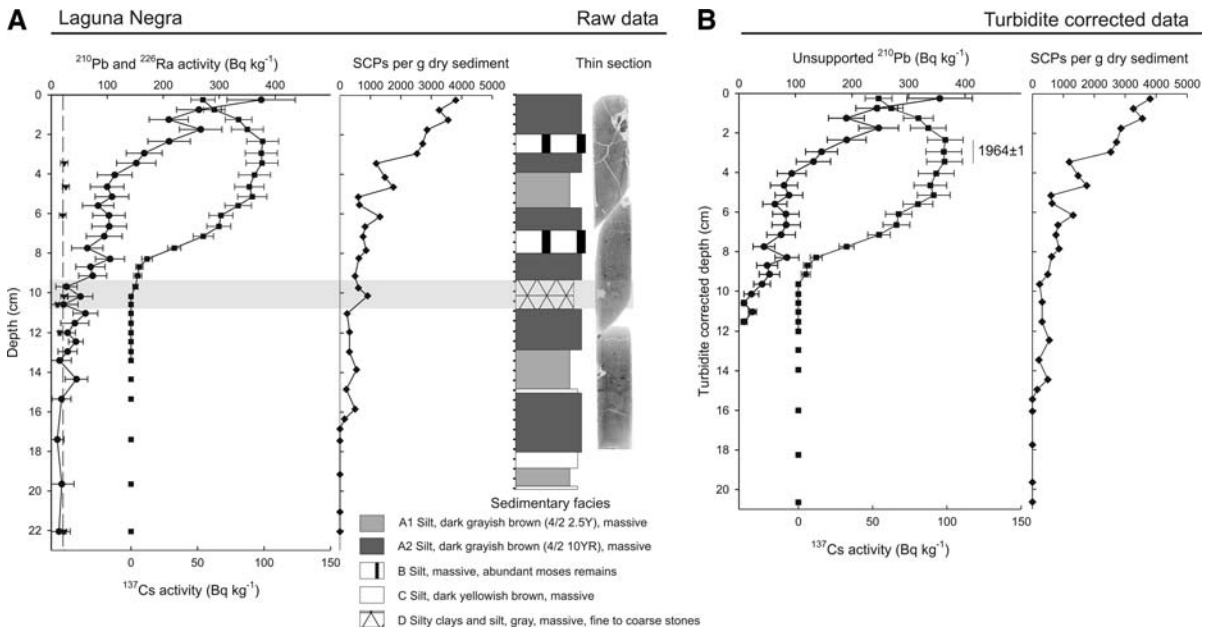

Fig. 2 **a** Total ^{226}Ra (triangles), ^{210}Pb (dots) and ^{137}Cs (squares) activity measurements, SCP concentrations and sediment facies of the short core from Laguna Negra. The turbidite is present between 9.4 and 10.8 cm of sediment depth. **b** Turbidite-corrected profiles for unsupported ^{210}Pb (dots) and ^{137}Cs (squares) activity. The maximum ^{137}Cs activity is recorded between 2.0 and 3.7 cm depth

profile is expected around that time. This is consistent with an SCP profile of Laguna Aculeo (33°50′S/70°54′W, 350 m a.s.l.) directly adjacent to Santiago, where the first SCPs have been dated to AD 1857 ± 6 (von Gunten et al., unpublished data).

Laguna El Ocho

Laguna El Ocho (34°02′S/70°19′W, 3250 m a.s.l.), situated 80 km south-east from Santiago (Fig. 1), is a small (15 ha), 45-m deep meromictic cirque lake with monomictic to dimictic water circulation in the mixolimnion. It is oligotrophic and has in the mixolimnion a pH of 6.6, an specific conductance of 133 μS cm^{-1} and a dissolved oxygen content of 7.4 mg l^{-1}. The monimolimnion has a pH of 7.0, an specific conductance of 787 μS cm^{-1} and dissolved oxygen content of 0.9 mg l^{-1}. The catchment has very steep slopes, ranges up to 3,800 m a.s.l., and consists mainly of volcanic Miocene rocks (andesites to basalt). The catchment is free of vegetation.

Four facies were identified in the sediment core of Laguna El Ocho (Fig. 3). Facies A consists of grayish brown and gray (5/2 10YR, 6/1 7.5YR), very finely laminated, very fine to medium silt. Bioturbation can be excluded. Facies B consists of greyish brown and gray (5/2 10YR, 6/1 7.5YR), fine to medium laminated very fine to medium silt. Facies C is composed of greyish brown and gray (5/2 10YR, 6/1 7.5YR), massive very fine to medium silt. Facies D is made of greyish brown to gray (5/2 10YR, 6/1 7.5YR), massive very fine to medium silt, with fine to medium stones.

The atmospheric pollution history of Laguna El Ocho is dominated be the local Cu mine El Teniente, the World's largest underground Cu mine, located windward from the lake further down-valley. Due to the mean synoptic wind regime, the influence of the megacity Santiago to the NW is minimal. Industrial mining started at El Teniente in the late end of the 19th century. The first smelter operated from AD 1904 onwards, and large-scale smelting started AD 1907 and AD 1909 (Jara 2005). Thus, first continuous SCP deposition in Laguna El Ocho did not occur before the beginning of the 20th century but should be placed around AD 1907 or AD 1909. A diagnostic peak in excess atmospheric Cu deposition (indicated by Cu/Rb) was identified at 2.25 cm sediment depth (Fig. 3): the significant decrease (despite increasing Cu production) reflects precisely the commissioning

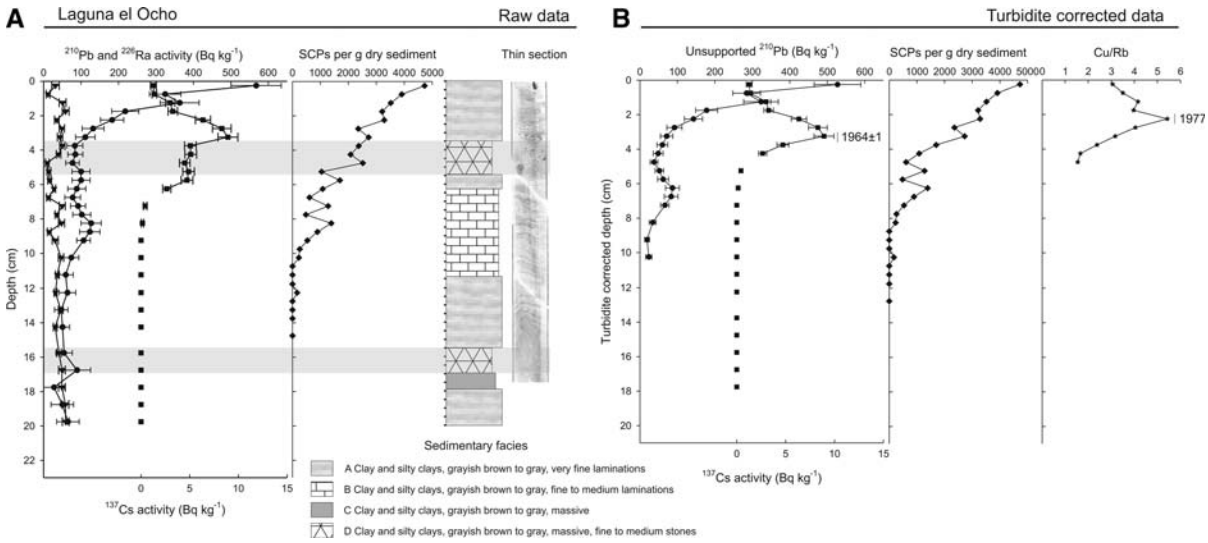

Fig. 3 **a** Total ^{226}Ra (triangles), ^{210}Pb (dots) and ^{137}Cs (squares) activity measurements, SCP concentrations and sediment facies of the short core from Laguna El Ocho. Two turbidites are present between 3.5 and 5.5 cm and 15.5 and 17.5 cm sediment depth. **b** Turbidite corrected profiles for unsupported ^{210}Pb (dots) and ^{137}Cs (squares) activity. The maximum ^{137}Cs activity is recorded at 3.25 cm depth. First SCPs occur at 12.25 cm; the continuous record starts at 10.25 cm sediment depth. The peak in the Cu/Rb (excess atmospheric Cu deposition) record at 2.25 cm sediment depth corresponds to the year AD 1977

of a new smelting technique and mineral dust recovery at El Teniente mine in the year AD 1977 (von Gunten et al., unpublished data).

Methods

In 2006, we retrieved short sediment cores with an UWITEC gravity corer equipped with action hammer in the deepest part of Laguna El Ocho (42 m water depth) and at 79 m water depth in Laguna Negra (Fig. 1). Cores were stored cold at 5°C until opened.

Prior to sampling for ^{210}Pb activity measurements, we prepared thin sections for sedimentary microfacies analysis using a four-component synthetic resin mixture (64% NSA, 25% VCD, 10% DER and 1% DMAE) in order to detect sections with rapid sedimentation (e.g., turbidites) that need to be removed from the ^{210}Pb activity profile (Arnaud et al. 2002). Subsequently, we used continuous sampling at irregular intervals according to the sedimentary microfacies for ^{210}Pb activity measurements. In Laguna Negra, we used a sampling interval between 0.4 and 0.7 cm, and in Laguna El Ocho, a sampling interval of 0.5 cm matched well with the limits of visible turbidites. This allowed us to precisely remove turbidite layers without loosing unsupported ^{210}Pb in the total activity of the profile.

Spheroidal carbonaceous particle (SCP) samples were prepared after Renberg and Wik (1985; H_2O_2 30% and HCl 10%), and were counted under a stereomicroscope at 50× magnification (Grob 2008).

Gamma-decay counts of ^{210}Pb (46.5 keV), ^{226}Ra (352 and 609 keV) and ^{137}Cs (662 keV) were collected for more than 20 h using Canberra low background, well-type GeLi-detectors at EAWAG, Dübendorf. We calculated the unsupported ^{210}Pb activity with the level-by-level method from the ^{226}Ra activity (Appleby and Oldfield 1978; Appleby 2001) in Laguna El Ocho. In Laguna Negra, the mean ^{226}Ra activity (20.3 Bq kg^{-1}) was used to account for the supported ^{210}Pb activity (Krishnaswamy et al. 1971) as ^{226}Ra activities were partially below the detection limit.

We tested the CFCS, CIC, CRS and SIT models on the turbidite-corrected ^{210}Pb profiles. The CFCS model assumes that both the flux of unsupported ^{210}Pb to the sediment and the sedimentation rate are constant. The CIC model assumes that the surface sediment $^{210}Pb_{unsupp}$ activity (A_0) is constant in time, and in consequence, the sedimentation rate may vary. The CRS model in contrast assumes that the flux of

$^{210}Pb_{unsupp}$ to the sediment remains constant and sedimentation rate may vary in time. The SIT model (Carroll and Lerche 2003) does not have *a priori* assumptions.

The SIT model uses inverse numerical analysis techniques in combination with a predictive activity module to reproduce the $^{210}Pb_{unsupp}$ profile. Non-exponential changes in the $^{210}Pb_{unsupp}$ activity that are caused either by changes in the sedimentation rate and/or in ^{210}Pb source processes are modelled by Fourier series (Carroll et al. 1995, 1999a). The values of the Fourier coefficients are determined for the measured data by inverse numerical analysis, which results in a mathematical expression that describes changes in the ^{210}Pb activity with sediment depth (Carroll et al. 1995; Carroll and Lerche 2003). The software for SIT calculation is documented in Carroll and Lerche (2003) (software kindly provided by J. Carroll, Polar Environmental Centre, Norway).

The CFCS, CIC and CRS model calculations were carried out as presented in Appleby (2001). When the CRS model was constrained with a time marker, we used the "composite CRS" method as described in Appleby (2001) and Appleby (pers. commun. 2007). Standard error calculation followed Appleby (2001) for the CRS model and Binford (1990) for the CIC model.

^{210}Pb age-depth models were first validated using the regional ^{137}Cs fallout peak of AD 1964 ± 1 (The Environmental Measurements Laboratory 2008). As a second stratigraphic horizon, we used the first occurrence of anthropogenic SCP fallout to the sediments, which corresponds to the onset of industrial and urban fossil fuel burning in the area of the lakes (Rose 2001). The first appearance of SCPs in a sediment record mirrors the local-to-regional industrial and urban history because the atmospheric transport of larger SCPs is limited (Rose 2001).

A further stratigraphic marker for Laguna El Ocho comes from a diagnostic peak in excess atmospheric Cu fallout, which is related to the production and processing history of the local Cu mine El Teniente. Excess atmospheric Cu was calculated from the Cu/Rb ratios in the sediments. Pre-industrial values for the Cu/Rb ratio were considered as natural background, and Rb is used as a proxy for allochthonous siliciclastic input to the sediments. Cu and Rb were measured with X-ray fluorescence (von Gunten et al., unpublished data). Turbidites and seismites were used as precise stratigraphic markers for historical earthquakes (Chapron et al. 2007).

Results and interpretation

Laguna Negra

Sedimentological characterization and thin sections showed the occurrence of a turbidite between 9.4 and 10.8 cm (Facies D, Fig. 2). Total ^{210}Pb reached equilibrium with ^{226}Ra at 12.0 cm sediment depth. ^{137}Cs showed highest values between 2.0 and 3.7 cm, and comprises the chronomarker horizon of AD 1964 ± 1.

As expected, the different models provided substantially different chronologies (Fig. 4). The CFCS, the un-constrained CRS and un-constrained SIT models yielded much younger ages and were not consistent with the ^{137}Cs peak. These models had to be rejected. The CIC model exhibited multiple large age inversions and is also rejected.

The constrained CRS and the constrained SIT models (both forced through the ^{137}Cs marker AD 1964) gave internally consistent results between AD 2006 and AD 1910 but diverged significantly (between 20 and 40 years) in the 2nd half of the 19th century (Fig. 4b).

First SCPs appeared at 16.4 cm (Fig. 2), which corresponds to a maximum age of AD 1857 ± 6 (see Sect. 3). The age of AD 1854 ± 9 at 12 cm depth, as suggested by the constrained CRS model is, therefore, much too old. Linear extrapolation of the lowermost three data points would suggest an unrealistic age of ca. AD 1730 for the first appearance of SCPs at 16.4 cm depth. The constrained CRS model overestimates sediment ages for the bottom part of the profile. This effect is not visible, however, if the CRS model is verified with the AD 1964 ^{137}Cs peak only. The constrained SIT model provides plausible ages for the bottom part of the profile (AD $1894^{+30}/_{-4}$ at 12 cm depth). Linear extrapolation of the constrained SIT ages places the first occurrence of SCPs at AD $1853^{+30}/_{-4}$, which is consistent with the urban history of Santiago.

The constrained SIT (constrained CRS) model assigns an age of AD $1906^{+25}/_{-4}$ (AD 1891 ± 9) to the turbidite at 9.4–10.8 cm depth. The constrained SIT age for the turbidite is consistent with the

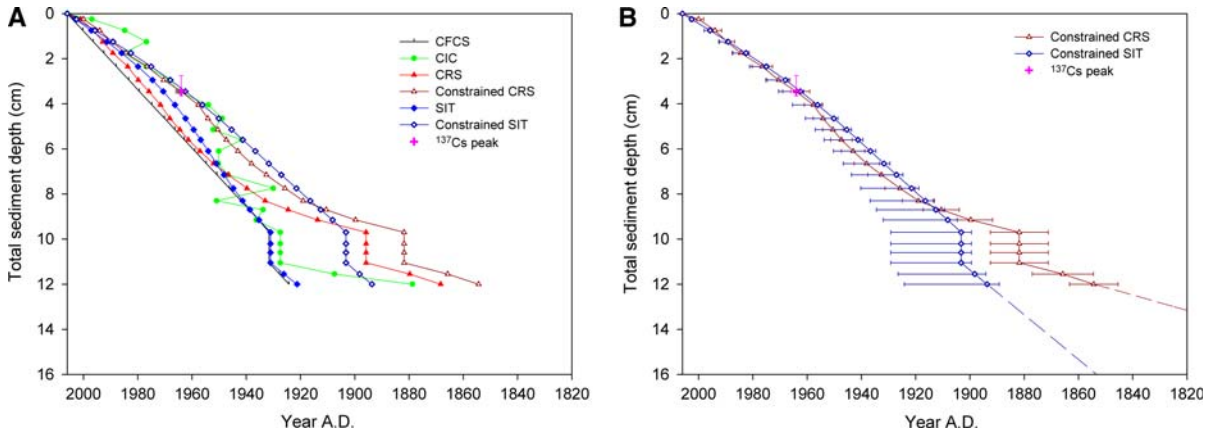

Fig. 4 Shows the comparison of the ^{210}Pb-based depth-to-age models for Laguna Negra. **a** Shows the mean values for all tested models (error bars are not given to enhance the readability). **b** Shows the ^{137}Cs-AD1964-constrained CRS and constrained SIT models with the dating uncertainty

earthquake of AD 1906 (Mw 8.2), while the constrained CRS model overestimated the age of the turbidite. No large earthquake was observed in that region between AD 1850 (Mw 7.3) and AD 1906 (Barrientos 2007; Servicio sismologico de Chile 2008).

Laguna El Ocho

Sedimentological characterization and thin sections show the occurrence of two turbidites between 3.5 and 5.5 cm, and between 15.5 and 17.5 cm (Facies D, Fig. 3). Total ^{210}Pb activity reaches equilibrium with ^{226}Ra activity at 13.5 cm total sediment depth. ^{137}Cs activity peaks sharply at 3.25 cm, which corresponds to the AD 1964 ± 1 chronomarker. The first SCPs are observed at 12.25 cm sediment depth, and continuous SCP records are found above 10.25 cm.

Both the CFCS and CIC model ages are not consistent with the ^{137}Cs AD 1964-bomb peak (Fig. 5a), and the CIC chronology shows multiple age inversions. Both models need to be rejected. The un-constrained CRS model yields ages for the ^{137}Cs (AD 1964) marker that are approximately 6 years too old. The un-constrained SIT model reproduces the ^{137}Cs bomb peak at AD 1964 very well and yields very consistent ages with the constrained SIT model (forced through AD 1964) over the entire dating

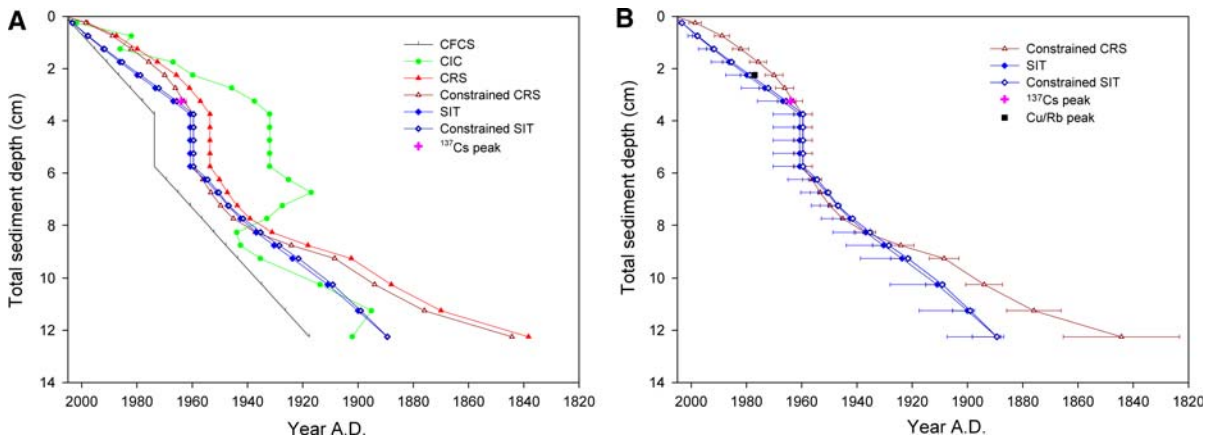

Fig. 5 Shows the comparison of the ^{210}Pb-based depth-to-age models for Laguna El Ocho. **a** Shows the mean values for all tested models (error bars are not given to enhance the readability). **b** Shows the ^{137}Cs-AD1964-constrained CRS and the constrained SIT models with the dating uncertainty

period (AD 1890–AD 2006). However, the constrained SIT model shows much smaller dating uncertainties ($\pm 1\sigma$ is approximately 50% reduced compared with the un-constrained SIT model).

Both SIT models and the constrained CRS model yield consistent chronologies for the middle section of the profile (between AD 1930 and AD 1964). In the upper part of the profile, the constrained CRS model shows approximately 10 years older ages compared with the SIT models (Fig 5b). In the lower part of the profile, however, the constrained CRS model is up to 45 years older than ages obtained with the SIT model.

For the bottom part of the profile prior to AD 1930, model validation with SCPs shows that both the unconstrained and the constrained CRS models overestimate the age of the onset of SCP fallout at Laguna El Ocho (AD 1844 ± 21 at 12 cm sediment depth, Fig. 5b). Both SIT models gave a plausible age for a first contamination with SCPs at 12.25 cm sediment depth (AD $1889^{+9}/_{-1}$) and for the continuous SCP record at 10.25 cm sediment depth (AD $1909^{+6}/_{-1}$), which corresponds in time with the onset of large-scale mining when smelters were put into operation.

For the top part between AD 1964 and AD 2006, the diagnostic Cu/Rb peak of AD 1977 clearly validates the SIT models (Fig. 5b) and reveals that the composite CRS model has a systematic offset of up to 10 years in this section.

Because the turbidite at 3.5–5.5 cm sediment depth in Laguna El Ocho is stratigraphically very close to the ^{137}Cs AD 1964 peak at 3.25 cm depth, it is not surprising that the constrained models (SIT and CRS) produce an age of AD 1960 for the turbidite that corresponds to the Great Chilean Earthquake of Valdivia (Barrientos 2007). The age of the turbidite at 15.5–17.5 cm sediment depth is more diagnostic for assessing the model choice. While the SIT models place this event into the AD 1850s, which corresponds to the 7.3 Mw historical earthquake of AD 1850, the CRS model suggests much older ages (mid-18th century).

Discussion

Our results show that there are significant differences between the ^{210}Pb-based chronologies. This finding is consistent with former studies (Appleby 2008), and it is influenced by the model applied and by cross-validation with independent chronostratigraphic markers.

As in many other studies, the bomb peak of ^{137}Cs is an important validation for the year AD 1964 ± 1 and helps constrain the models where this is numerically possible (CRS and SIT). Unfortunately, the AD 1986 ^{137}Cs peak is not present in the southern hemisphere, which implies that the section of the ^{210}Pb profile younger than AD 1964 cannot be validated with ^{137}Cs. The same is the case for the section prior to AD 1964 to the beginning of the ^{210}Pb profiles (end of the 19th century) where no radiochemical markers are available except, theoretically, ^{14}C wiggle matching (Blaauw et al. 2003). The long period prior to the ^{137}Cs AD 1964 peak (approx. 2/3 of the profile) is most important when long instrumental and observational data series (e.g., meteorological data) must be used for calibration and cross-validation of the lake sediment proxies.

Our results show that the SCP profiles in the sediments of Laguna Negra and Laguna El Ocho provide an objective criterion to detect inconsistencies and thus to reject the (constrained) CRS model, and to accept the (constrained) SIT model results. The first occurrence of SCPs in the sediment is an unambiguous indication that the sediment sample cannot be older than the onset of industrial activity in the region of the lake. In most parts of the World, the beginning of fossil fuel consumption and SCP deposition falls largely into the lower part of the ^{210}Pb chronologies. Thus we recommend that SCPs should be systematically investigated in the section of the sediment core, where unsupported ^{210}Pb disappears.

In both lakes, the CFCS and CIC models did not provide consistent results, which is in agreement with previous studies because in most lakes, the fundamental model assumptions are not met (Appleby 2001). The CIC model resulted in large time inversions because the ^{210}Pb profile is non-monotonic.

The unconstrained CRS model failed to reproduce the correct age for the ^{137}Cs bomb peak (AD 1964 ± 1) in both lakes and had to be constrained using the composite CRS method. In both lakes, the ages of the lowest samples calculated with the composite CRS model were grossly overestimated, which resulted in unrealistically old ages for the onset of regional SCP deposition. Overestimation of the

CRS ages at the bottom of ^{210}Pb profiles has been observed before (e.g., McCall et al. 1984; Turner and Delorme 1996; Carroll and Lerche 2003). This finding is particularly critical for climate reconstructions because calibration or cross-validation over the early period would significantly jeopardize the calibration or verification statistics, and ultimately result in very large errors of prediction for the down-core reconstructions (RMSEP, Cook et al. 1994).

In Laguna El Ocho, the composite CRS model overestimates sediment ages in the top 4 cm of the sediment core (stratigraphically above the ^{137}Cs AD 1964 peak) by as much as 10 years. This shows that independent validation of the topmost part is also very critical even if the model is constrained by the ^{137}Cs AD 1964 peak. This is especially true as the AD 1986 ^{137}Cs peak is missing in the Southern Hemisphere. An offset by 10 years is not acceptable for calibration with instrumental records because erroneous statistics would result for the most important frequency bands of decadal and multi-annual climate variability, such as the El Niño Southern Oscillation.

Whereas in Laguna Negra the SIT model had to be constrained using the ^{137}Cs AD 1964 peak to get a realistic chronology, both the un-constrained and constrained SIT model revealed plausible chronologies in Laguna El Ocho. In both lakes, validation with the SCP data showed that the constrained SIT model yielded plausible ages over the entire dating period, i.e., also for the bottom samples of the ^{210}Pb profile. The age of the bottom samples are in agreement with the regional and local industrial/urban history. In Laguna Negra, when sediment ages are extrapolated to a depth of 16.4 cm, the first occurrence of SCPs in the sediment is estimated to AD $1853^{+30}/_{-4}$, which is consistent with the data from Laguna Aculeo (AD 1857 ± 6, von Gunten et al., unpublished data), and the historical data for the onset of the industrial activity in the region of Santiago (AD 1850–1870). Although the cumulative probability distribution for sediment ages (P(10)–P(90)) of the SIT model is relatively large (Fig. 4b), the proximity of the most probable age P(68) to the P(90) limit implies little uncertainty at the 90% confidence value (Carroll and Lerche 2003).

Constraining the SIT model with the ^{137}Cs AD 1964 marker horizon resulted in reduced standard deviations of the model sediment ages. Reducing the standard deviation is critically important for correlation with instrumental records since the time series of proxy data needs to be smoothed to account for dating errors before calibration with independent (meteorological) data is possible (Koinig et al. 2002). The minimum smoothing factor is determined by the largest standard deviation of the age model. This explains why the standard deviation of the calibration chronology is directly related to the maximum temporal resolution of the calibration and reconstruction. This is most critical if decadal or inter-annual climate variability (e.g., ENSO) is the target of the research. In consequence, constraining the SIT model should always be applied. It is noteworthy that the numerical design and the software of the SIT model allow easily for the assimilation of additional chronological information with individual uncertainties.

Systematic testing of the models reveals which sections of chronologies are most robust. Largest discrepancies between the CRS and SIT model in Laguna Negra and Laguna El Ocho occur in the bottom part of the profile (late 19th century), while the chronologies are consistent and very robust in the middle (Laguna El Ocho AD 1930–1964) or upper part of the profile (Laguna Negra AD 1964–2006).

Conclusions

We investigated how high-precision, well-validated chronologies with reduced uncertainty of young (last 100–150 years) non-varved lake sediments can be achieved. Our approach included (i) irregularly-spaced sampling for ^{226}Ra, ^{210}Pb and ^{137}Cs activity counting, (ii) a systematic comparison of numerical models for the calculation of ^{210}Pb-based chronologies (CFCS, CIC, CRS and SIT), (iii) constraining the CRS and SIT models with the ^{137}Cs marker of AD 1964 and (iv) step-wise cross-validation with independent diagnostic environmental stratigraphic markers of known age. Stratigraphic markers in this study included airborne pollutants such as SCPs, excess atmospheric Cu deposition, and turbidites related to historical earthquakes. In other settings, other types of chronomarkers, such as flood or tephra layers, seismites or turbidites, pollen of invasive species, charcoal from historical forest fires, etc., could be used. These chronomarkers help to evaluate the different model chronologies and to select the

best model for a given lake. In general, much more emphasis should be placed on such independent markers.

Our results from two high-elevation lakes in the Central Chilean Andes show that the ^{137}Cs (AD 1964)-constrained SIT model performs significantly better than the CFCS, CIC and CRS models. Our results also confirm that the CRS model tends to overestimate sediment ages in the lower part of the ^{210}Pb profile (beginning of the 20th century, end of the 19th century), which is particularly critical if long periods of instrumental data need to be covered for calibration and cross-validation purposes.

Reducing the standard deviations (SD) of chronology is important because the SD of sediment ages is proportional to the temporal resolution at which sedimentary proxy data can be calibrated in time. Very small SDs are absolutely critical if inter-annual climate phenomena, such as, e.g., ENSO, are quantitatively studied from lake sediment data.

We recommend systematic testing to confirm the general validity of our conclusions in a wide variety of lakes, sediment types, and catchment configurations.

Acknowledgements We thank J. Carroll and P.G. Appleby for valuable communications; A. Zwyssig for technical assistance; A. Araneda, I. Alvial, H. Alonso (all from EULA Concepción, Chile) and C. Nazal (CODELCO, Chile) for their help during the 2006 field campaign; Aguas Andinas, CODELCO and DIFROL for permission to conduct research. E. Grieder made the radiometric measurements and R. Krisai identified the *fissidens* water moos. T. Whitmore is acknowledged for the careful editorial help. This project is funded by the Swiss National Science Foundation (NF-200021-107598 and 200020-121869).

References

Abril JM (2004) Constraints on the use of ^{137}Cs as a time-marker to support CRS and SIT chronologies. Environ Pollut 129:31–37. doi:10.1016/j.envpol.2003.10.004

Albrecht A, Reiser R, Luck A, Stoll JMA, Giger W (1998) Radiocesium dating of sediments from lakes and reservoirs of different hydrological regimes. Environ Sci Technol 32:1882–1887. doi:10.1021/es970946h

Appleby PG (2000) Radiometric dating of sediment records in European mountain lakes. J Limnol 59(suppl. 1):1–14

Appleby PG (2001) Chronostratigraphic techniques in recent sediments. In: Last WM, Smol JP (eds) Tracking environmental change using lake sediments. Volume 1: Basin analysis, coring and chronological techniques. Kluwer Academic Publishers, Dordrecht, The Netherlands, pp 171–201

Appleby PG (2008) Three decades of dating recent sediments by fallout radionuclides: a review. Holocene 18:83–93. doi:10.1177/0959683607085598

Appleby PG, Oldfield F (1978) The calculation of lead-210 dates assuming a constant rate of supply of unsupported ^{210}Pb to the sediment. Catena 5:1–5. doi:10.1016/S0341-8162(78)80002-2

Appleby PG, Oldfield F, Thompson R, Huttunen P, Tolonen K (1979) Pb-210 dating of annually laminated lake-sediments from Finland. Nature 280:53–55. doi:10.1038/280053a0

Arnaud F, Lignier V, Revel M, Desmet M, Beck C, Pourchet M, Charlet F, Trentesaux A, Tribovillard N (2002) Flood and earthquake disturbance of Pb-210 geochronology (Lake Anterne, NW Alps). Terra Nova 14:225–232. doi:10.1046/j.1365-3121.2002.00413.x

Barrientos SE (2007) Earthquakes in Chile. In: Moreno T, Gibbons W (eds) The geology of Chile. The Geological Society, London, pp 263–287

Binford MW (1990) Calculation and uncertainty analysis of ^{210}Pb dates for PIRLA project lake sediment cores. J Paleolimnol 3:253–267. doi:10.1007/BF00219461

Birks HJB (1998) Numerical tools in palaeolimnology—progress, potentialities, and problems. J Paleolimnol 20:307–332. doi:10.1023/A:1008038808690

Blaauw M, Heuvelink GBM, Mauquoy D, van der Plicht J, van Geel B (2003) A numerical approach to ^{14}C wiggle-match dating of organic deposits: best fits and confidence intervals. Quat Sci Rev 22:1485–1500. doi:10.1016/S0277-3791(03)00086-6

Blass A, Grosjean M, Troxler A, Sturm M (2007) How stable are twentieth-century calibration models? A high-resolution summer temperature reconstruction for the eastern Swiss Alps back to AD 1580 derived from proglacial varved sediments. Holocene 17:51–63. doi:10.1177/0959683607073278

Boës X, Fagel N (2008) Relationships between southern Chilean varved lake sediments, precipitation and ENSO for the last 600 years. J Paleolimnol 39:237–252. doi:10.1007/s10933-007-9119-9

Bradley RS, Briffa KR, Cole JE, Hughes MK, Osborn TJ (2003) The climate of the last millenium. In: Alverson K, Bradley RS, Pedersen F (eds) Paleoclimate, global change and the future. Springer, Berlin, pp 105–141

Carroll J, Lerche I (2003) Sedimentary processes: quantification using radionuclides. Elsevier, Oxford

Carroll J, Lerche I, Abraham JD, Cisar DJ (1995) Model-determined sediment ages from Pb-210 profiles in unmixed sediments. Nucl Geophys 9:553–565

Carroll J, Lerche I, Abraham JD, Cisar DJ (1999a) Sediment ages and flux variations from depth profiles of Pb-210: lake and marine examples. Appl Radiat Isot 50:793–804. doi:10.1016/S0969-8043(98)00099-2

Carroll J, Williamson M, Lerche I, Karabanov E, Williams DF (1999b) Geochronology of Lake Baikal from Pb-210 and Cs-137 radioisotopes. Appl Radiat Isot 50:1105–1119. doi:10.1016/S0969-8043(98)00116-X

Chapron E, Juvigne E, Mulsow S, Ariztegui D, Magand O, Bertrand S, Pino M, Chapron O (2007) Recent clastic sedimentation processes in Lake Puyehue (Chilean Lake District, 40.50 degrees S). Sediment Geol 201:365–385. doi:10.1016/j.sedgeo.2007.07.006

Color M (1994) Munsell soil color charts. Macbeth Division of Kollmorgen Instruments Corporation, New Windsor

Cook ER, Briffa KR, Jones PD (1994) Spatial regression methods in dendroclimatology—a review and comparison of 2 techniques. Int J Climatol 14:379–402. doi:10.1002/joc.3370140404

Grob P (2008) Spheroidal carbonaceous particles SCPs als Indikatoren der Umweltbelastung und als Datierungsmethode junger Seesedimente. MSc Thesis. University of Bern, Bern

Hegerl G, Crowley TJ, Hyde WT, Frame DJ (2006) Climate sensitivity constrained by temperature reconstructions over the past seven centuries. Nature 440:1029–1032. doi:10.1038/nature04679

Jara AEV (2005) History of mining in Chile (Part 3). CIM Bull 98:119–121

Jones PD, Mann ME (2004) Climate over past millennia. Rev Geophys 42:1–42. doi:10.1029/2003RG000143

Koinig KA, Kamenik C, Schmidt R, Gusti-Panareda A, Appleby PG, Lami A, Prazakova M, Rose N, Schnell OA, Tessadri R, Thompson R, Psenner R (2002) Environmental changes in an alpine lake (Gossenkollesee, Austria) over the last two centuries—the influence of air temperature on biological parameters. J Paleolimnol 28:147–160. doi:10.1023/A:1020332220870

Krishnaswamy S, Lal D, Martin JM, Meybeck M (1971) Geochronology of lake sediments. Earth Planet Sci Lett 11:407–414. doi:10.1016/0012-821X(71)90202-0

Liu J, Carroll JL, Lerche I (1991) A technique for disentangling temporal source and sediment variations from radioactive isotope measurements with depth. Nucl Geophys 5:31–45

Luterbacher J, Dietrich D, Xoplaki E, Grosjean M, Wanner H (2004) European seasonal and annual temperature variability, trends, and extremes since 1500. Science 303:1499–1503. doi:10.1126/science.1093877

Mamalakis MJ (1976) The growth and structure of the Chilean economy: from independence to Allende. Yale University Press, London

McCall PL, Robbins JA, Matisoff G (1984) Cs-137 and Pb-210 transport and geochronologies in urbanized reservoirs with rapidly increasing sedimentation-rates. Chem Geol 44:33–65. doi:10.1016/0009-2541(84)90066-4

McCormac FG, Hogg AG, Blackwell PG, Buck CE, Higham TFG, Reimer PJ (2004) SHCal04 Southern hemisphere calibration, 0–11.0 cal kyr BP. Radiocarbon 46:1087–1092

Miller A (1976) The climate of Chile. In: Schwerdtfeger W (ed) Climates of Central and South America. Elsevier, Amsterdam, pp 113–146

Moberg A, Sonechkin DM, Holmgren K, Datsenko NM, Karlen W (2005) Highly variable Northern Hemisphere temperatures reconstructed from low- and high-resolution proxy data. Nature 433:613–617. doi:10.1038/nature03265

Moernaut J, De Batist M, Charlet F, Heirman K, Chapron E, Pino M, Brummer R, Urrutia R (2007) Giant earthquakes in South-Central Chile revealed by Holocene mass-wasting events in Lake Puyehue. Sediment Geol 195:239–256. doi:10.1016/j.sedgeo.2006.08.005

Oldfield F, Appleby PG, Battarbee RW (1978) Alternative Pb-210 dating—results from New-Guinea highlands and Lough Erne. Nature 271:339–342. doi:10.1038/271339a0

Ortega L (1981) Acerca de los origenes de la industrializacion Chilena, 1860–1879. Nueva Hist 1:3–54

Pennington W, Cambray RS, Fisher EM (1973) Observations on lake sediments using fallout Cs-137 as a tracer. Nature 242:324–326. doi:10.1038/242324a0

Renberg I, Wik M (1984) Dating recent lake sediments by soot particle counting. Int Verein Limnol 22:712–718

Renberg I, Wik M (1985) Soot particle counting in recent lake sediments. An indirect dating method. Ecol Bull 37:53–57

Rippy JF, Pfeiffer J (1948) Notes on the dawn of manufacturing in Chile. Hisp Am Hist Rev 28:292–303. doi:10.2307/2507747

Ritchie JC, Mchenry JR, Gill AC (1973) Dating recent reservoir sediments. Limnol Oceanogr 18:254–263

Robbins JA (1978) Geochemical and geophysical applications of radioactive lead. In: Nriagu JO (ed) The biogeochemistry of lead in the environment. Wiley, New York, pp 285–377

Rose NL (2001) Fly-ash particles. In: Last WM, Smol JP (eds) Tracking Environmental change using lake sediments. Volume 2: Physical and geochemical methods. Kluwer Academic Publishers, Dordrecht, pp 319–349

Rose NL, Harlock S, Appleby PG (1999) The spatial and temporal distributions of spheroidal carbonaceous fly-ash particles (SCP) in the sediment records of European mountain lakes. Water Air Soil Pollut 113:1–32. doi:10.1023/A:1005073623973

Servicio sismologico de Chile (2008) Sismos importantes y/o destructivos (1570—Mayo 2005). Universidad de Chile, Santiago

Sonke JE, Burnett WC, Hoogewerff JA, van der Laan SR, Vangrosveld J, Corbett DR (2003) Reconstructing 20th century lead pollution and sediment focusing in a peat land pool (Kempen, Belgium), via Pb-210 dating. J Paleolimnol 29:95–107. doi:10.1023/A:1022858715171

The Environmental Measurements Laboratory (2008) SASP measurements database. U.S. Department of Homeland Security, New York

Turner LJ, Delorme LD (1996) Assessment of Pb-210 data from Canadian lakes using the CIC and CRS models. Environ Geol 28:78–87. doi:10.1007/s002540050080

Waugh WJ, Carroll J, Abraham JD, Landeen DS (1998) Applications of dendrochronology and sediment geochronology to establish reference episodes for evaluations of environmental radioactivity. J Environ Radioact 41:269–286. doi:10.1016/S0265-931X(98)00002-2

Zolitschka B, Mingram J, van der Gaast S, Jansen JHF, Naumann R (2001) Sediment logging techniques. In: Last WM, Smol JP (eds) Tracking environmental change using lake sediments. Volume 1: Basin analysis, coring and chronological techniques. Kluwer Academic Publishers, Dordrecht, The Netherlands, pp 137–154